PHENIX Experiment at RHIC

M. Rosati
Iowa State University, Ames, IA 50011, USA
E-mail: mrosati@iastate.edu

for the PHENIX Collaboration

The primary goal of the PHENIX collaboration is the detection and characterization of the quark-gluon plasma. We will outline the capabilities of the PHENIX experiment for measuring leptonic decays of the J/ψ and other quarkonium states.

1 Introduction

The Relativistic Heavy Ion Collider (RHIC), being built at Brookhaven National Laboratory, will offer a unique opportunity for detecting and subsequently characterizing the quark-gluon plasma by comparing nuclear collisions of a range of species and at a variety of beam energies. It will be an important task for the PHENIX collaboration to clarify the mechanisms of quarkonium suppression. We will be able to exploit the flexibility of the RHIC accelerator which can provide both proton and heavy ion beams at different energies. In the following sections, we will outline the capabilities of the PHENIX experiment in measuring J/ψ, ψ' and Υ through their decays into e^+e^- and $\mu^+\mu^-$. Measuring a variety of quarkonium states, characterized by different values of the meson radius, in pp, pA, AA collisions will enable us to make a systematic study of vector meson production and disentangle the hadronic and QGP contributions to the suppression.

2 The PHENIX Detector

The PHENIX experiment will look for a variety of expected signatures of the quark-gluon plasma. It is designed as a high rate detector to measure signatures of deconfinement and color screening, chiral symmetry restoration, thermal radiation of a hot gas, strangeness and charm production, and space time evolution of the plasma. The experimental plan is to measure lepton, photon, and hadron production as a function of various external variables such as mass of colliding ions and energy density in heavy ion collisions.

The PHENIX detector[3] will have four spectrometers as shown in Figure 1. Around the interaction region, a silicon multiplicity/vertex detector will measure charged particles for -2.5 $\leq \eta \leq$ 2.5 and full range in azimuth (ϕ). It will provide a good measurement of centrality in heavy ion collision, from which

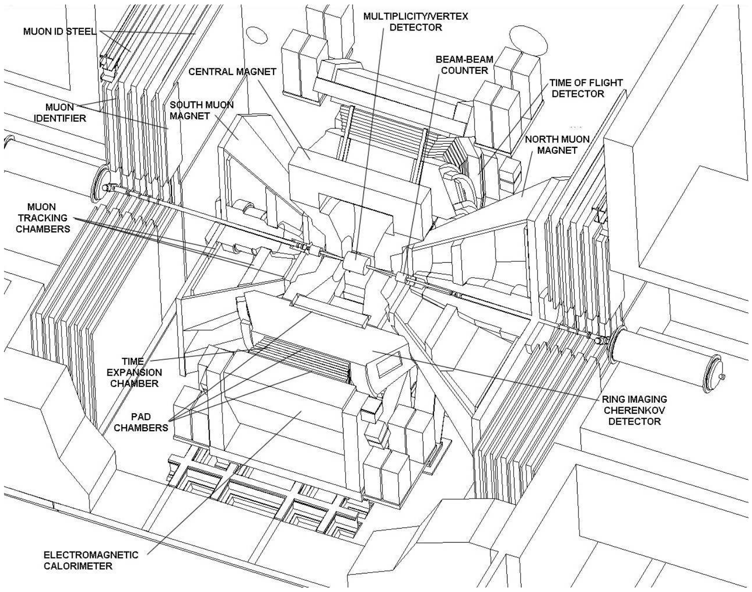

Figure 1: Detector Layout of the PHENIX Experiment.

the energy density can be inferred. At midrapidity there are two arms, with axial magnetic field, covering an interval of ± 0.35 units of rapidity and $180°$ in ϕ. At forward rapidities there are two radial field muon spectrometers covering the rapidity range $1.2 \leq |y| \leq 2.5$ and full azimuth. The PHENIX detector will cover a selective acceptance, as shown in Figure 2, using multiple detector technologies to achieve very discriminating particle identification.

Each Central Arm contains three tracking subsystems: Drift Chambers (DC) measuring accurately in r-ϕ, Pixel Pad Chambers (PC) determing space points, and Time Expansion Chambers (TEC) providing tracking and particle identification by dE/dx measurements. In addition, various particle identification devices are installed, such as a ring imaging Cherenkov detector (RICH), Time-of-Flight (TOF) system and an electromagnetic calorimeter (EMCAL). The RICH detector is filled with ethane at atmospheric pressure with a readout of phototubes arrays located near the magnet pole tips. The TOF detector will cover half the azimuth of the East Central Arm and will be used to identify hadrons. Given the timing resolution of 80 ps, it will enable us to separate pions from kaons up to a transverse momentum of 2 GeV/c. The EMCAL utilizes two technologies: one quarter is made of Pb-Glass, while the rest is

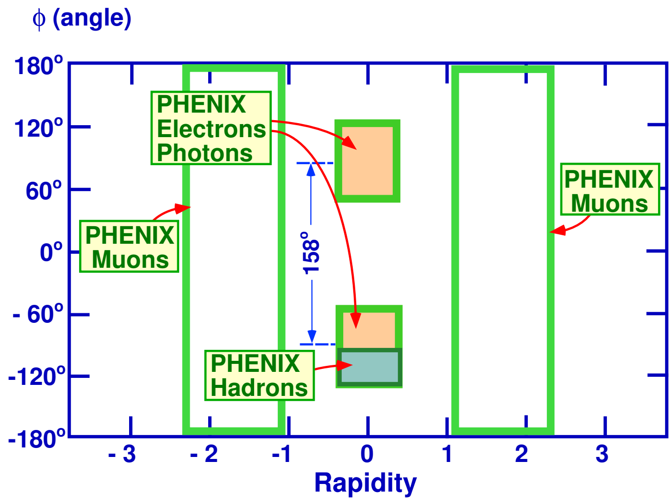

Figure 2: The Acceptance Regions of the PHENIX Central and Muon Arms.

a Pb-Scintillator sampling calorimeter. They have excellent energy resolution and are instrumented with timing readout which will allow hadron identification in the central arm region not covered by the TOF detector.

The Muon Arms are comprised of a set of absorber materials to keep most of the hadrons that are produced at the interaction region from reaching the detection chambers. Following the absorber materials are two conical shaped magnets which provide a radial magnetic field over a region of approximately 4 meters in the z direction. Inside these magnets are three stations of tracking devices with three planes of Cathode Strip Chambers (CSCs) each characterized by a position resolution of 100 μm per plane. Following the muon tracking systems are Muon Identifiers consisting of 6 gaps interleaved with 5 layers of steel. The gaps are instrumented with Iarocci streamer tubes and will be used to trigger and identify muons.

3 Electron Measurements

Vector mesons decaying into dileptons will appear as peaks in the invariant mass plot. Since heavy ion collisions at RHIC will produce high charged particle densities (dN/dy$\sim$ 1000), it is essential to have good particle identification to minimize the combinatorial background. In particular, particles misidentified as electrons could give rise to spurious e^+e^- pairs which might look like

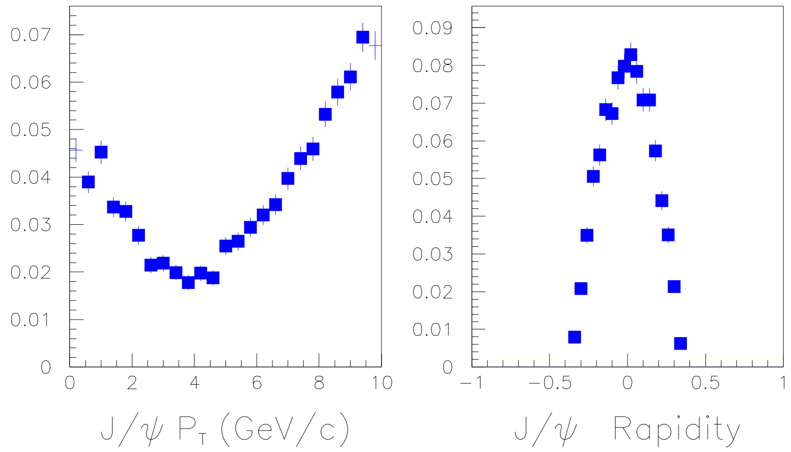

Figure 3: The acceptance for $J/\psi \to e^+e^-$ detection in the PHENIX Central Arms as a function of rapidity and transverse momentum.

the signal of interest.

Charged particles are reconstructed as tracks in the Central Arm tracking system. The trajectory information combined with the vertex information, provide a measurement of the particle momentum. Electrons are identified by using 3 detector elements: the RICH, the EMCAL and the TEC. Electrons are identified in the RICH by associating tracks with the Cherenkov photon rings. The electron-hadron rejection factor, achieved with this method, has been measured in a beam test to be at the level of 10^{-4}. In a higher multiplicity enviroment the RICH is expected to provide a rejection factor of 500. An additional discrimation of between electron and hadrons is provided by the dE/dx deposited in the Time Expansion Chamber with a rejection factor of 10. The EMCAL provides electron identification by matching the energy deposited in the calorimeter and the momentum measured with the tracking. This will provide a further rejection factor of 20-30.

The J/ψ acceptance was calculated as the ratio of number of J/ψ's decaying into e^+e^- going through the PHENIX electron arms to the total number of produced J/ψ's. A plot of the acceptance as a function of the J/ψ rapidity and transverse momentum is shown in Figure 3.

The invariant mass resolution was also evaluated to be 20 MeV/c^2 and it has a weak dependence on the J/ψ momentum as shown in Figure 4A.

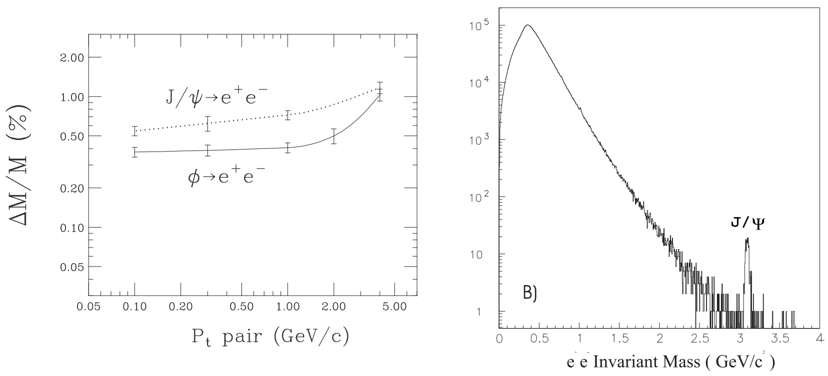

Figure 4: A) Expected Invariant Mass Resolution for for $J/\psi \rightarrow e^{+}e^{-}$ detection as a function of the pair transverse momentum, B) Simulation of invariant mass spectrum for central Au-Au Collisions for all $e^{+}e^{-}$ pairs

The dielectron invariant mass spectrum resulting from a full simulation of the PHENIX detector is shown in Figure 4B for 32 M events corresponding to roughly one week of RHIC running at full luminosity. The J/ψ peak is well distinguished from the background, which is mostly due to $e^{+}e^{-}$ pairs originating from photon conversions and Dalitz decays.

4 Muon Measurements

Vector meson production can also be measured through their decay into $\mu^{+}\mu^{-}$ pairs. The information of the Cathode Strip Chambers is used, along with the vertex position from the MVD, to reconstruct particle momenta at the vertex. The separation of pions from muons is achieved by requiring that muons have matching tracks in the tracking and identification systems and by comparing the depth that a particle reaches in the identification system with the momentum that is measured in the tracking system. The minimum energy of an identifiable muon will be 2 GeV/c and the expected pion rejection factor is 10^{-4}.

The J/ψ acceptance was calculated as the ratio of the number of J/ψ's decaying into $\mu^{+}\mu^{-}$ going through the PHENIX muons spectrometer to the total number of J/ψ's. A plot of the acceptance as a function of the J/ψ rapidity and transverse momentum is shown in Figure 5. A clear advantage of this detection method is a gain in yield of a factor of ~ 10, since the $\Delta y \Delta \phi$ coverage of the muon spectrometers is a factor of 3 larger than for the central arms. The invariant mass resolution was also evaluated to be 105 MeV/c^{2} for

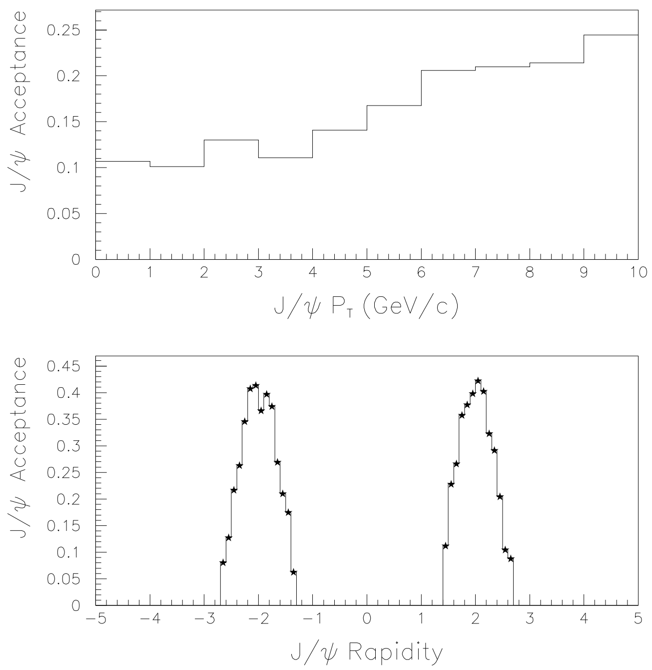

Figure 5: The acceptance for $J/\psi \rightarrow \mu^+\mu^-$ in the PHENIX Muon Arms as a function of rapidity and transverse momentum.

J/ψ and ψ' and 180 MeV/c for the Υ resonances.

The dimuon invariant mass spectrum resulting from a full simulation of the PHENIX detector is shown in Figure 6, for the integrated luminosity expected at RHIC in a nominal one year of running. The J/ψ peak is well distinguished from the background with a signal to background ratio of 7:1. The ψ' peak is also visible and has a signal to background ratio of 0.4:1. The muon arms will provide vector meson measurement for masses ranging from the ϕ to the Υ and will extend our rapidity coverage. Furthermore the electron and muon arms cover regions of phase space with different hadron density and therefore will provide an ideal environment to evaluate the modification of the J/ψ cross section in the hadronic medium.

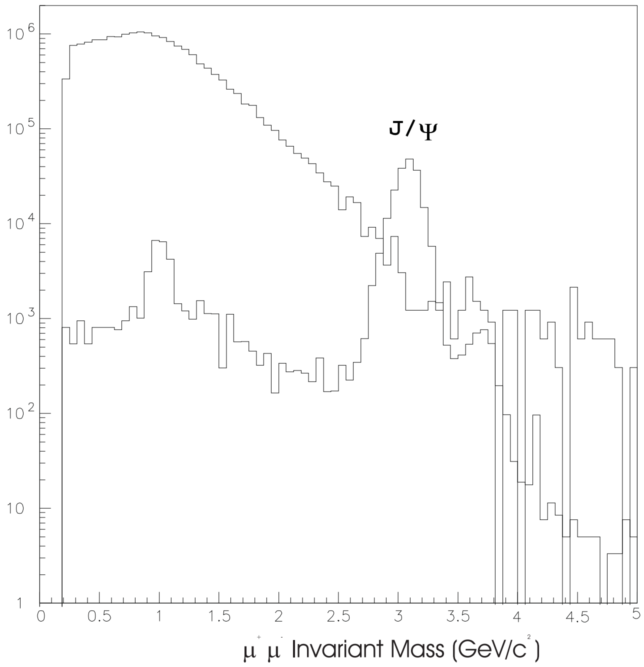

Figure 6: Simulation of the invariant mass spectrum for central Au-Au collisions for all $\mu^+\mu^-$ pairs: signals of vector mesons, Drell Yan pairs and charm production are shown separately from the combinatorial background.

5 Integrated Acceptances and Yields

To estimate the expected quarkonium cross section we use the results of the next-to-leading order calculation in the color evaporation model [4], which has been shown to agree with existing data on J/ψ production in proton-proton and proton-nucleus collisions.

The J/ψ cross section in proton-proton collision at $\sqrt{s}$=200GeV/c^2 is estimated to be:

$$\sigma_{pp \to J/\psi} = 3.3\mu b$$

The branching fraction of J/ψ into dileptons has been measured [5] to be:

$$BR(J/\psi \to e^+e^-) = BR(J/\psi \to \mu^+\mu^-) = (6.0 \pm 0.2)\%$$

Using the differential cross section predicted by this model, we estimate

Table 1: Integrated Acceptance for Vector Mesons.

Particle	Decay Mode	Acceptance (%)
J/ψ	$\mu^+\mu^-$	8.6
ψ'	$\mu^+\mu^-$	8.6
Υ	$\mu^+\mu^-$	8.3
J/ψ	e^+e^-	0.75
ψ'	e^+e^-	0.75

the integrated acceptance for the various vector meson states detected through their dimuon and dielectron decays as shown in Table 1.

The integrated J/ψ cross section in proton-nucleus collisions shows a depedence which can be parametrized by a power law:

$$\sigma_{pA \to J/\psi} = A^{\alpha} \sigma_{pp \to J/\psi}$$

where the α exponent characterizes all the nuclear effects. The E772 collaboration has studied J/ψ production extensively on nuclear targets [1] and has measured α=0.92.

To estimate the J/ψ production rate in Au-Au collisions at RHIC we assume that no anomalous suppression [2] is present and that the nuclear effect can be accounted for with the following parametrization:

$$\sigma_{AA \to J/\psi} = A^{2\alpha} \sigma_{pp \to J/\psi}$$

Using these assumptions our estimate of J/ψ production rate in Au-Au collisions at RHIC is:

$$\sigma_{AA \to J/\psi} BR(J/\psi \to dileptons) = 3.3mb$$

The RHIC design luminosity is $2 \cdot 10^{26} cm^{-2} s^{-1}$ for Au-Au collisions, assuming that the data taking period will be 8 months/year and accounting for 50 % detector and accelerator down time, we estimate that 2.6 million J/ψ's per year will be produced at RHIC. Similar calculations can be made for all quarkonium states and, accounting for the PHENIX detector acceptance, we determined the expected yields for vector mesons as shown in Table 2. These yields are comparable to the data sample collected in experiment E 772 at Fermilab[1], which has done the most precise studies of J/ψ production so far. Within one year of running at full luminosity PHENIX will be able to accurately measure J/ψ yields and the challenge will be to disantangle the various physics contributions to the production.

Table 2: Vector Meson Expected Yields

Particle	Decay Mode	Minimum Bias Yield
J/ψ	$\mu^+\mu^-$	530K
ψ'	$\mu^+\mu^-$	9K
Υ	$\mu^+\mu^-$	0.8K
J/ψ	e^+e^-	46K
ψ'	e^+e^-	0.8K

6 Summary

Within one year of RHIC running at full luminosity, the PHENIX experiment will have a J/ψ sample size comparable to the NA50 experiment. PHENIX has a unique ability of measuring several quarkonium states thus allowing the comparison of states with very different binding radii. In addition, RHIC will produce pp, pA and AA collisions, therefore we expect to be able to perform a systematic study of charmonium and bottomoniun production which will provide stringent constraints on the theoretical models of J/ψ production and suppression.

7 Acknowledgments

This work was supported by the U.S. Department of Energy Grant DOE-FG02-92ER40692 and a grant from Iowa State University.

References

1. D.M. Alde et al. *Phys. Rev. Lett.* **66**, 63 (1991).
2. M.Gonin et al. *Nucl. Phys.* A **610**, 404 (1996), M.C. Abreu et al. PLB **410**, 327 (1997).
3. PHENIX Conceptual Design Report, BNL 1993 (unpublished), Y. Akiba et al., *Nucl. Phys.* A **638**, 565 (1998)
4. R. Gavai et al. *Int. J. Mod. Phys.* A **10**, 3043 (1995).
5. Particle Data Group, *Eur. Phys. J.* **3**, 583 (1998).